

# SEISMIC BEHAVIOR OF MASONRY BUILDINGS

by

Pedro A. Hidalgo,<sup>1</sup> and Hugh D. McNiven<sup>2</sup>

## ABSTRACT

Experiments have been conducted to evaluate the seismic behavior of window piers typical of high-rise masonry construction. Sixty-three fixed ended piers were subjected to cyclic, in-plane shear loads. Principal test parameters were the type of masonry construction, the height-to-width ratio, the amount of reinforcement and the effect of full and partial grouting. An identification of the principal modes of failure is presented. Also included is a proposition to predict the ultimate strength associated with the shear mode of failure on the basis of the experimental data, as it becomes available. Finally, the effect of the test parameters on the inelastic characteristic of piers exhibiting the shear mode of failure is discussed.

## INTRODUCTION

This paper describes the main findings of a masonry research program that has been carried since 1972 at the Earthquake Engineering Research Center of the University of California, Berkeley. The first objective of this program is to carry out an experimental study on the inelastic seismic behavior of structural components of shear walls typical of multistory masonry buildings (Fig. 1). The second is to use the experimental data to formulate mathematical models of the inelastic behavior of the structural elements for inclusion in computer programs. These computer programs permit the prediction of the response of multistory masonry buildings to ground earthquake excitation.

Two structural elements can be found in the shear wall panels shown in Fig. 1, the piers and the spandrel beams. The results presented herein only refer to the experimental phase of the research program associated with piers. Initially, a pilot series of seventeen concrete block double pier panels were tested as shown in Fig. 2. Deep spandrel beams at both top and bottom of the piers prevented the rotation of the end sections of the piers. These tests were intended to study the effect of rate of loading, bearing load and types of reinforcing on the inelastic behavior of the piers [1]. The test results [2] validated other results on cantilever piers [3] showing that piers failing in the flexural mode of failure have desirable inelastic behavior. It was also concluded that the rate of loading does not have a significant effect on the ultimate strength of the piers and consequently a low cyclic frequency was adopted for the rest of that program. Moreover, the results demonstrated the need for more extensive tests on piers failing in the shear mode, in order to establish definitive parametric relationships.

---

<sup>1</sup> Visiting Associate Research Engineer, Earthquake Engineering Research Center (EERC), University of California, Berkeley, California.

<sup>2</sup> Professor of Engineering Science, University of California, Berkeley, Calif.

The cost of the double pier tests, both in time and money, precluded carrying out the extensive parametric study using this test procedure, and consequently a single pier system was devised (Fig.3), which greatly simplified the investigation. In this test setup, two hinged external steel columns restrain the rotation of the top of the pier, forcing it towards the same condition of rotation fixity at top and bottom sections that was developed in the double pier test system (Fig. 2). The parameters of the sixty-three single pier tests included the type of masonry material, the height-to-width ratio of the piers, the type of grouting and the amount of horizontal reinforcement. The test results of the single pier test program have been reported in detail elsewhere [4,5]. This paper presents the major conclusions on how the parameters mentioned above affect the ultimate shear strength and the inelastic behavior of the piers.

Although the bearing load was not included as one of the parameters of the single pier test program, the value of the compressive vertical load acting on the pier increased as the in-plane horizontal displacement of the test specimen increased, due to the natural tendency of the steel columns to maintain a constant length (Fig. 3). This circumstance distorted the results in two ways; first, it changed the mode of failure of some of the piers, and second, the inelastic behavior of the piers, after the major diagonal cracks have occurred, may be different from the behavior observed in the tests reported here. These conclusions have been validated by preliminary tests carried out using a modified single pier test setup that eliminated the additional compressive load on the piers. The modification consisted of replacing the steel columns by vertical actuators; these actuators are commanded to impose forces of equal value but opposite sign at two sides of the pier and the magnitude of the forces is selected to maintain the point of inflection of the deformed shape at the mid-height of the pier. The modified single pier test setup permits the test to be developed under any desired constant bearing load and a series of tests is presently under way to ratify or modify the results concerning the inelastic behavior of the piers after major diagonal cracks have occurred.

#### TEST PROGRAM AND TEST PROCEDURE

Three types of masonry material were used throughout the pier test program, namely hollow concrete block (HCBL), hollow clay brick (HCBR) and double wythe grouted core clay brick piers (CBRC). The HCBL piers were constructed from standard two-core reinforceable hollow concrete blocks, nominally 8 in. (20 cm) wide by 8 in. (20 cm) high by 16 in. (40 cm) long. The HCBR piers were constructed from standard two-core reinforceable hollow clay bricks, nominally 8 in. (20 cm) wide by 4 in. (10 cm) high by 12 in. (30 cm) long. The CBRC piers were constructed from two wythes of solid clay brick units, nominally 4 in. (10 cm) wide by 4 in. (10 cm) high by 12 in. (30 cm) long; the grouted core between the two wythes was nominally 2 in. (5 cm) thick giving the test specimens a thickness of 10 in. (25 cm).

The test program included single piers with three height-to-width ratios. Piers HCBR-21 and CBRC-21 were 80 in. (2.03 m) high by 42 in. (1.07 m) wide, with a height-to-width ratio of 1.90. Piers HCBL-11, HCBR-11 and CBRC-11 were 56 in. (1.42 m) high by 48 in. (1.22 m) wide, with a height-to-width ratio of 1.17. The piers with height-to-width ratio of 0.5 (HCBL-12, HCBR-12 and CBRC-12) were 40 in. (1.02 m) high by 80 in. (2.03 m) wide.

Two types of grouting were used in the HCBR-11, HCBR-11 and HCBR-21 piers; in the partially grouted piers only the cells and the bond beams containing reinforcement were grouted; the fully grouted piers had all the cells grouted. All of the other piers were fully grouted.

The test equipment shown in Figs. 2 and 3 permits lateral loads to be applied in the plane of the piers, using displacement controlled actuators with a maximum capacity of 450 kip (203 ton). A vertical load may be applied to the piers through the spring and rollers shown above the spandrel beam in Fig. 2 and above the lateral loading beam in Fig. 3. All the single pier tests had an initial bearing stress of 50 psi (3.5 kg/cm<sup>2</sup>). The lateral loading sequence for each test consisted of sets of three sinusoidal displacement cycles applied at a specified actuator displacement amplitude. The specified amplitude was gradually increased and followed a sequence that varied according to the height-to-width ratio of the piers. The cyclic frequency was generally maintained at 0.02 Hz.

The basic product obtained from the tests was the hysteresis loops diagram, which is a plot of the lateral load against the lateral displacement of the piers as shown in Fig. 4. The strength and deformation properties, the stiffness degradation and the energy dissipation characteristics of the piers can be obtained from the hysteresis loops. The hysteresis envelope, also shown in Fig. 4, is a plot of the absolute average of the maximum positive and negative forces and corresponding displacements, for each of the three cycles of loading at a given input displacement amplitude.

#### MODES OF FAILURE

Two principal modes of failure have been observed during the tests, a flexural and shear mode. Sliding modes associated with either shear or flexural crack were also observed in the piers with height-to-width ratio of 0.5.

A flexural mode of failure was obtained in two of the double pier tests (HCBL-21) and in the preliminary tests using the modified single pier test setup. The specimens have only horizontal cracks at the top and bottom sections and the ultimate strength of the pier is controlled by the tensile yielding strength of the vertical reinforcement. In this case the final mechanism of failure is due to crushing at the compressive toe of the pier.

Most of the piers exhibited a shear mode of failure. This mode is characterized by early flexural cracks at the toes of the pier which are later augmented by diagonal cracks that extend through a partial zone of the pier. As the horizontal load increases, large diagonal cracks (X cracks) form when the diagonal tensile stress in the pier reaches the tensile strength capacity of the masonry. Some of the single piers with height-to-width ratio of 2 or 1 exhibited yielding in the vertical reinforcement before the occurrence of the major diagonal cracks. However, as the vertical compressive load induced by the single pier test setup (Fig. 3) increased, the flexural moment capacity of the pier sections also increased while the tension vertical reinforcement continued to yield. This effect allowed the lateral load on the pier to increase until the diagonal tensile stress reached the tensile strength of the masonry and a shear failure developed. The same test was later repeated using the modified single pier test setup and a typical flexural mode of failure was obtained. This fact shows how important the compressive axial load may be in shifting the mode of failure from the flexural to shear.

## ULTIMATE STRENGTH ASSOCIATED WITH THE SHEAR MODE OF FAILURE

The ultimate lateral load strength of each pier is determined by the lesser of the lateral load capacities associated with each of the modes of failure. The ultimate strength associated with the two sliding modes of failure described above proved to be quite similar to that obtained with the shear mode of failure.

The lateral load capacity associated with the flexural mode of failure is reasonably predicted by current analytical methods, which can be found in reference [2].

The lateral load capacity associated with the development of the first major diagonal crack (shear strength), will be analyzed in detail using the experimental data obtained throughout the test program. This lateral load capacity usually, but not always [4], coincides with the ultimate (maximum) shear strength of the piers.

Figure 5 presents a comparison between the experimental shear strength of the piers and the allowable shear stress that the pier would have according to the Uniform Building Code (UBC), 1979 Edition. Both the percentage of horizontal reinforcement and the axial stress developed concurrently with the major diagonal crack have been used as parameters, even though the axial force effect is not considered by the UBC. The code allowable shear stress is also a function of the compressive strength of the corresponding masonry prism and the height-to-width ratio of the piers (or  $M/Vd$ ). Both effects have proved to be significant factors to the shear capacity of the piers. Except for unreinforced or very lightly reinforced piers, the allowable stress given by the UBC appears to be a good basis to predict the shear strength of masonry piers.

Based on the previous result, Fig. 6 presents the experimental shear strength as a function of  $v_{n,r}$ , which is the basic expression proposed by the UBC to evaluate the allowable shear stress of an unreinforced pier. Fig. 6 illustrates the improvement in strength that can be obtained through the use of horizontal reinforcement and the beneficial effect of compressive load on the shear strength. As more experimental data becomes available, it will be possible to predict with more confidence the shear strength of masonry piers. Fig. 7 presents the same data separated by masonry material. It is interesting to observe the different effect of the horizontal reinforcement depending on the type of masonry.

## INELASTIC BEHAVIOR OF PIERS FAILING IN THE SHEAR MODE

In order to simplify the analysis, the inelastic characteristics of the piers exhibiting a shear mode of failure are discussed using the area A of the hysteresis envelope, as defined in Fig. 8. The area A is directly proportional to the ultimate strength and the ductility developed by the piers, but other parameters like the energy dissipated per cycle and the comparison of crack patterns at equal displacements must be considered to fully evaluate the inelastic characteristics of the pier behavior.

Figure 9 presents the effect of horizontal reinforcement and height-to-width ratio on the inelastic behavior of the piers. It can be observed that increasing amounts of horizontal reinforcement improve the inelastic behavior; however, this improvement is not large and presents more consistency for the HCBL and HCBR piers than for the CBRC piers. The squat piers (height-to-width

ratio of 0.5) generally show better inelastic behavior than the more slender piers.

The effect of partial grouting as compared with full grouting is shown in Fig. 10, using shear forces for the comparison. The behavior of partially grouted HCBL piers is not significantly less desirable than that of fully grouted piers, but definitively worse in the case of the HCBR piers.

#### SUMMARY OF RESULTS

1. Two principal modes of failure may occur in a masonry pier, flexure and shear. In addition, the piers with height-to-width ratio of 0.5 showed a tendency to develop a sliding mode of failure.
2. The strength associated with the shear mode of failure is a function of the compressive strength of the masonry material and the ratio  $M/Vd$  of the pier. This strength may be improved with increasing amounts of horizontal reinforcement and increasing values of the compressive axial load acting on the pier.

#### ACKNOWLEDGEMENTS

The research reported in this paper has been jointly funded by the National Science Foundation, the Masonry Institute of America, the Western States Clay Products Association and the Concrete Masonry Association of California and Nevada. The sponsorship of these institutions is gratefully acknowledged.

#### REFERENCES

- [1] Mayes, R. L., Omote, Y. and Clough, R. W., "Cyclic Shear Tests of Masonry Piers, Volume I - Test Results", EERC Report No. 76-8, University of California, Berkeley, California, 1976.
- [2] Mayes, R. L., Omote, Y. and Clough, R. W., "Cyclic Shear Tests of Masonry Piers, Volume II - Analysis of Test Results", EERC Report No. 76-16, University of California, Berkeley, California, 1976.
- [3] Priestley, M.J.N. and Bridgemann, D.O., "Seismic Resistance of Brick Masonry Walls", Bulletin of the New Zealand National Society for Earthquake Engineering, Vol. 7, No. 4, 1974.
- [4] Hidalgo, P. A., Mayes, R. L., McNiven, H. D., and Clough, R. W., "Cyclic Loading Tests of Masonry Single Piers, Volume I - Height to Width Ratio of 2", EERC Report No. 78/27, University of California, Berkeley, California, 1978.
- [5] Hidalgo, P. A., Mayes, R. L., McNiven, H. D., and Clough, R. W., "Cyclic Loading Tests of Masonry Single Piers, Volume 3 - Height to Width Ratios of 0.5", EERC Report No. 79/12, University of California, Berkeley, California, 1979.

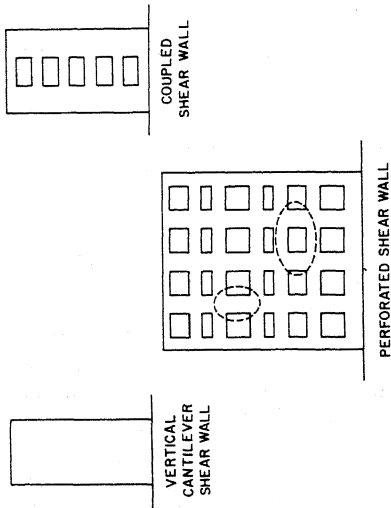


FIG. 1. TYPICAL SHEAR WALLS.

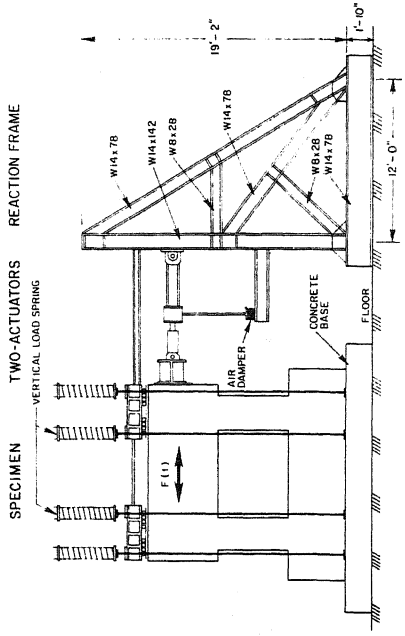


FIG. 2 DOUBLE PIER TEST SETUP

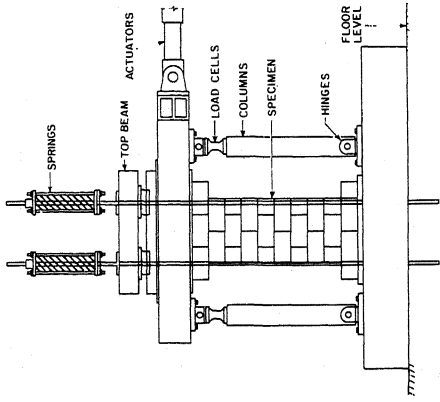


FIG. 3 SINGLE PIER TEST SETUP

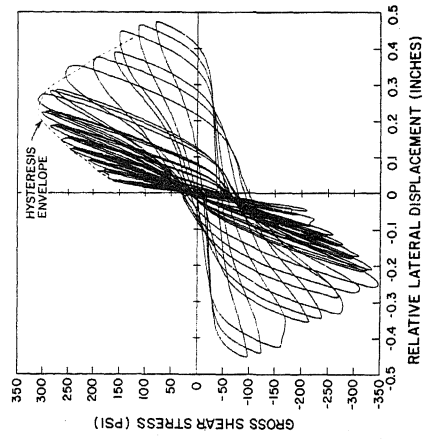


FIG. 4 HYSTERESIS LOOPS AND HYSTERESIS ENVELOPE

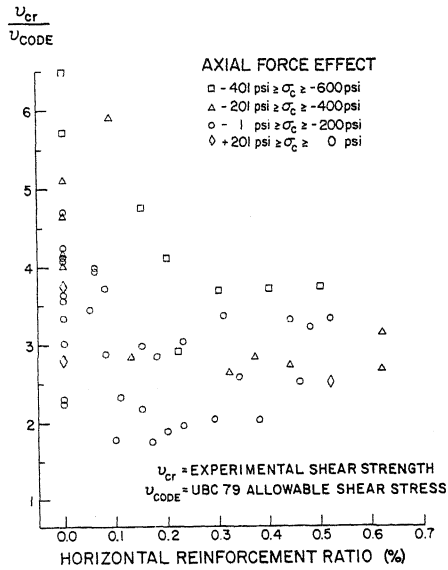


FIG. 5 COMPARISON BETWEEN EXPERIMENTAL SHEAR STRENGTH AND UBC 1979 ALLOWABLE SHEAR STRESS

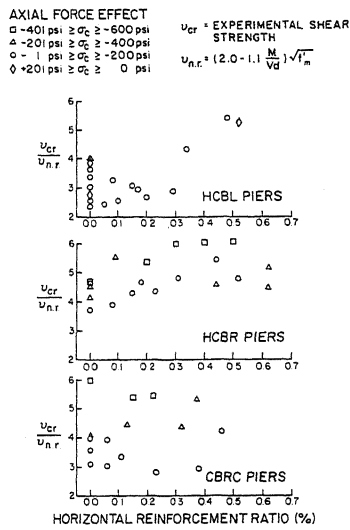


FIG. 7 EFFECT OF HORIZONTAL REINFORCEMENT AND AXIAL FORCE ON SHEAR STRENGTH OF MASONRY PIERS

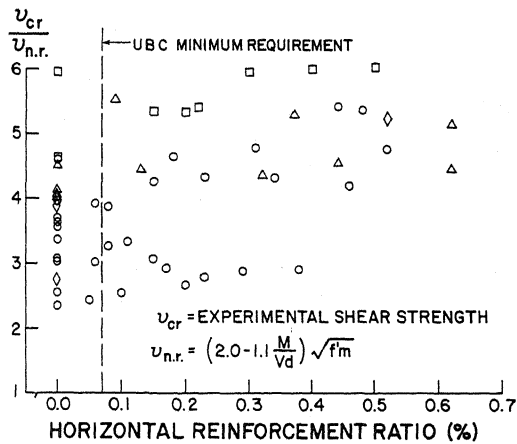


FIG. 6. EFFECT OF HORIZONTAL REINFORCEMENT AND AXIAL FORCE ON SHEAR STRENGTH OF MASONRY PIERS.

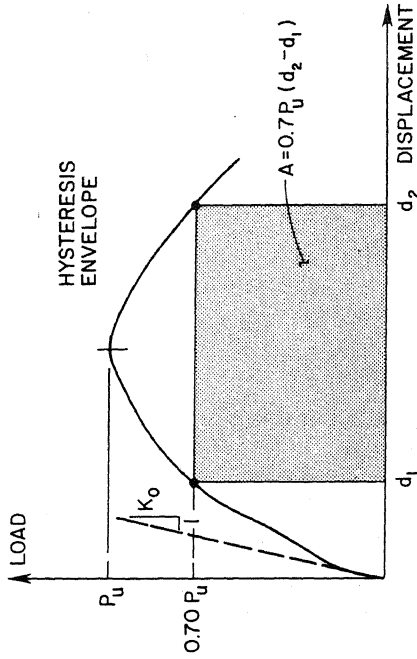


FIG. 8. DEFINITION OF PARAMETER A.

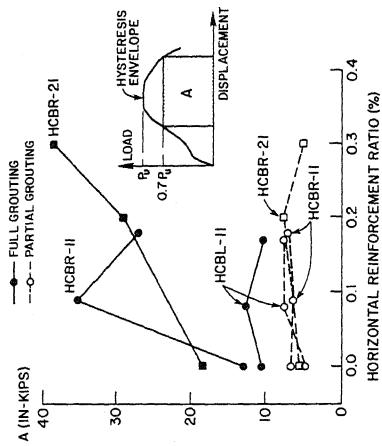


FIG. 10. EFFECT OF TYPE OF GROUTING ON INELASTIC BEHAVIOR OF PIERS.

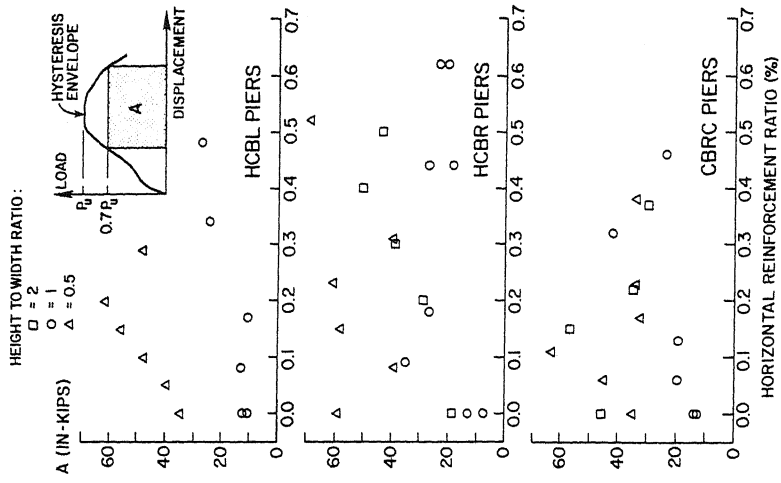


FIG. 9. EFFECT OF HORIZONTAL REINFORCEMENT AND HEIGHT-TO-WIDTH RATIO ON INELASTIC BEHAVIOR OF PIERS.